
RAD4XCNN: A NEW AGNOSTIC METHOD FOR *post-hoc* GLOBAL EXPLANATION OF CNN-DERIVED FEATURES BY MEANS OF RADIOMICS

Francesco Prinzi¹, Carmelo Militello^{2,*}, Calogero Zarcaro¹, Tommaso Vincenzo Bartolotta¹, Salvatore Gaglio^{3,2}, and Salvatore Vitabile¹

¹Department of Biomedicine, Neuroscience and Advanced Diagnostics, University of Palermo, Palermo, 90127, Italy

²Institute for High-Performance Computing and Networking (ICAR-CNR), National Research Council, Palermo, 90146, Italy

³Department of Engineering, University of Palermo, Palermo, 90128, Italy

*Corresponding author: email: carmelo.militello@cnr.it

April 26, 2024

ABSTRACT

-Background and Objective: In recent years, machine learning-based clinical decision support systems (CDSS) have played a key role in the analysis of several medical conditions. Despite their promising capabilities, the lack of transparency in AI models poses significant challenges, particularly in medical contexts where reliability is a mandatory aspect. However, it appears that explainability is inversely proportional to accuracy. For this reason, achieving transparency without compromising predictive accuracy remains a key challenge. **Methods:** This paper presents a novel method, namely Rad4XCNN, to enhance the predictive power of CNN-derived features with the inherent interpretability of radiomic features. Rad4XCNN diverges from conventional methods based on saliency maps, by associating intelligible meaning to CNN-derived features by means of Radiomics, offering new perspectives on explanation methods beyond visualization maps. **Results:** Using a breast cancer classification task as a case study, we evaluated Rad4XCNN on ultrasound imaging datasets, including an online dataset and two in-house datasets for internal and external validation. Some key results are: *i*) CNN-derived features guarantee more robust accuracy when compared against ViT-derived and radiomic features; *ii*) conventional visualization map methods for explanation present several pitfalls; *iii*) Rad4XCNN does not sacrifice model accuracy for their explainability; *iv*) Rad4XCNN provides a global explanation enabling the physician to extract global insights and findings. **Conclusions:** Our method can mitigate some concerns related to the explainability-accuracy trade-off. This study highlighted the importance of proposing new methods for model explanation without affecting their accuracy.

Keywords Explainable AI · Radiomics · Convolutional Neural Networks · Breast Cancer · Clinical Decision Support Systems

1 Introduction

The use of computer-aided tools based on Artificial Intelligence (AI) methods has increased significantly. These tools utilize machine learning and deep learning architectures in many types of Decision Support Systems (DSS). A particular class of DSS is represented by Clinical decision support systems (CDSS), implemented to support activities in critical healthcare processes. Although data-driven methods play a crucial role in CDSSs development, their use in medicine still harbors many pitfalls. New deep learning methods and the growing data availability have enabled the development of powerful but uninterpretable CDSS, and, for this reason, the field of Explainable AI (XAI) has gained considerable

attention. Regulatory authorities have discussed the lack of explainability Kundu [2021], Arrieta et al. [2020]. The US Federal Trade Commission emphasizes that AI tools should be transparent, explainable and fair Smith [2020]. The European Parliament has adopted the General Data Protection Regulation (GDPR), in which meaningful explanations of the logic involved are declared mandatory when automated decision-making is performed Guidotti et al. [2018]. Finally, with the Regulation (EU) 2024/1689 of the European Parliament, on July 2024 was approved the AI Act, establishing harmonized rules on the use of artificial intelligence-based systems European Community [2024]. In this perspective, the AI Act aims to achieve its stated policy objectives with a focus on transparency and human oversight Panigutti et al. [2023].

From a practical point of view, the lack of transparency makes both doctors and patients skeptical about these new technologies. Opaque AI systems can impair the doctor-patient relationship and jeopardize patient trust Amann et al. [2020]. For this reason, scientific research is working on making AI transparent and/or explainable Combi et al. [2022]. In medical contexts, several aspects can affect the model reliability and demand explainability Holzinger [2016], Holzinger et al. [2019]. Consequently, methods that enable transparency and explainability can help validate the models, improve the knowledge domain, and increase the use of these systems in the real world. For these reasons, although it is not yet fully accepted Bornstein [2016], Ghassemi et al. [2021], McCoy et al. [2022], London [2019], explainability is increasingly becoming a requirement that these systems should fulfill Jovanović and Schmitz [2022].

Deep learning architectures have demonstrated remarkable capabilities in extracting intricate patterns and features from huge datasets, enabling unprecedented predictive performance in various fields, including medical image analysis. Although deep features achieve impressive accuracy, the question of explainability is ignored and several approaches were proposed for their *post-hoc* explanation. These approaches focus mainly on visualization maps, which have shown several limitations regarding their reliability. As an example, applying different saliency map methods can result in different explanations Cerekci et al. [2024], Prinzi et al. [2024a], Zhang et al. [2022]. Furthermore, while saliency maps provide a form of local explanation, it has been shown that a global explanation is necessary for clinical model validation Prinzi et al. [2023a].

Radiomics Gillies et al. [2016], Lambin et al. [2017] is a new alternative approach to introduce explainability within the feature extraction process in radiological imaging Prinzi et al. [2024b]. Radiomic uses mathematical formulas to analyze grayscale histograms, ROI shapes, or texture-defining matrices. Consequently, each radiomic feature's significance is well known, and meaningful clinical conclusions can be drawn through model explanation Prinzi et al. [2024c]. In addition, radiomics is more suitable for training in small dataset scenarios. In fact, model training relies on algorithms designed for tabular data analysis, which are more appropriate for training with limited data An et al. [2021], Traverso et al. [2018]. Although radiomic features have the great properties of training in small data scenarios and inherent explainability, their predictive power seems considerably weaker than deep features, as has been shown in several works Lisson et al. [2022], Sun et al. [2020], Truhn et al. [2019], Wei [2021]. As a result, deep learning architectures are implemented when accuracy is the metric to maximize Truhn et al. [2019].

Considering that the feature extraction process from medical images represents the main step to implement high accuracy and explainability, several studies analyzed the interpretable capability of radiomic features Varriano et al. [2022] and the differences between learned features and radiomic features Rundo and Militello [2024]. The dilemma concerning the trade-off between explainability and accuracy arises van der Veer et al. [2021a]. Hence, the use of deep features would ensure highly performing but poorly explainable models, in contrast, radiomic features would ensure less accurate but interpretable models.

In this study, we combine the predictive power of deep features with the intrinsic explainability characteristic of radiomic features. To this aim, state-of-the-art architectures such as ResNet, DenseNet, and Vision Transformer (ViT) for deep feature extraction were employed Rahman et al. [2024]. Simultaneously, a radiomic workflow to extract interpretable signatures was implemented. We performed a comparative analysis between these two feature sources in terms of predictive performance and explainability. Moreover, we propose Rad4XCNN, a new method leverages deep learning for enhanced performance while exploiting the inherent interpretability of radiomic features. In particular, from a methodological perspective, Rad4XCNN doesn't introduce constraints or bottlenecks that can harm accuracies in deep architecture training Alvarez Melis and Jaakkola [2018], Elbaghdadi et al. [2020] while it explains CNN-derived features by means of radiomics. From a clinical perspective, Rad4XCNN uses quantitative radiomic features for explanations, introduces a form of global explanation, enriches image interpretation with intelligible features, and contributes to improved reliability, consistency, and confidence in radiologic practices. In addition, it provides new perspectives on the development of explanation methods not solely relying on visualization maps Papanastasiou et al. [2023]. A breast cancer classification task was proposed as a case study to evaluate the effectiveness of Rad4XCNN. To this end, we acquired two in-house datasets, one for training and internal testing and the other for external validation.

The main contributions are:

- Rad4XCNN a new method able to explain deep features by means of radiomics;
- a comparison between deep and radiomic features in terms of explainability and accuracy, providing insights on the importance of proposing new methods to overcome the accuracy-explainability trade-off dilemma;
- the use of deep architectures for breast cancer classification in ultrasound imaging exploiting an online dataset, and two in-house datasets for internal test and external validation;

The rest of the article is structured as follows: Section 2 'Background' Section introduces the main concepts of explainable AI and focuses on methods for explaining deep architectures and radiomic models. Section 3 'Materials and Methods' describes the datasets and the methods implemented, including our novel approach for global explanation of deep features. Section 4 'Experimental Results' compares the results of deep architectures and radiomic models in terms of accuracy and explainability. Section 5 'Discussion' Section exposes the importance of our approach to obtain accurate and interpretable models. Finally, Section 6 'Conclusion' highlights the main results.

2 Background

The proposed method embraces the explainability problem by exploiting the advantages and disadvantages of deep learning and radiomic workflow-based classification methods. Therefore, the section introduces general concepts related to XAI and particularizes deep architectures and radiomics. At the end of the section, the need and importance of the proposed method are justified.

2.1 Explainable AI

Numerous definitions of explainable AI are not fully standardized yet Longo et al. [2024]. For this article, it is essential to delineate certain concepts. A model is *intrinsically interpretable* when its transparent structure allows an understanding of its decision process. For this reason, a transparent algorithm doesn't require explanation methods for its interpretation. From an algorithmic point of view, Logistic Regression, Decision Tree, and Naive Bayes are considered transparent, while Neural Networks-based methods are defined as *black-boxes*. In the case of black-box algorithms, explanation methods are required for their introspection. An explanation can be global and local. A *global explanation* focuses on explaining a model's behavior across its entire dataset. A *local explanation* explains the prediction of a specific dataset sample (*i.e.* patient). To an *intelligible feature* it is possible to associate a human-understandable meaning. Radiomic features are considered intelligible. On the other hand, *deep features* that are extracted using neural network-based architectures, lack interpretability (are not intelligible). We can call features extracted via convolutional neural networks *CNN-derived*, and extracted via Vision Transformer as *ViT-derived*.

The combination of intelligible features and transparent algorithms makes the whole system intrinsically interpretable for two reasons: 1) it is possible to calculate the impact of the feature for model decision; 2) it is possible to correlate and validate the model's findings comparing it with the clinical literature. Local and global explanations are possible by employing black-box algorithms and intelligible features. These techniques are usually implemented to the already trained model and are known as *post-hoc* algorithms. When not-intelligible features are used, model explainability becomes significantly more complex: model findings cannot be compared with clinical literature because each feature's meaning is unknown. A method is defined *agnostic* when can be applied to any algorithm and architecture. For classification tasks, an XAI method can be *class-dependent* when explanations are given for each class separately, conversely, they are defined as *class-independent*.

2.2 Explainability in Deep Architectures

Convolutional-based neural networks have emerged as a standard for deep feature extraction in medical images. Deep learning has shown outstanding capabilities in diagnostic imaging across various diseases and modalities, highlighting its potential as a valuable clinical tool. Despite this promise, its adoption in clinical settings remains limited. One of the main reasons is related to the lack of transparency and trust de Vries et al. [2023]. The idea of saliency maps, which is used to highlight the visual regions that are most important for the prediction, is the primary emphasis of these architectures' explainability Itti et al. [1998], Mamalakis et al. [2023]. In Simonyan et al. [2013], given an input image, the gradient computation of the class score is calculated to visualize the activation map for a particular class. Integrated gradients are proposed in Sundararajan et al. [2017] for a more robust explanation through activation maps, adding the constraint of respecting the '*sensitivity*' and the '*implementation invariance*' principles/axioms. In Zeiler et al. [2011] and Zeiler and Fergus [2014] a network using deconvolution is proposed to visualize the convolutional network while in Springenberg et al. [2014] the guided back-propagation is introduced to visualize the features learned from CNN. The most popular algorithms exploiting saliency belong to the category of 'class activation maps' (CAM) Zhou et al.

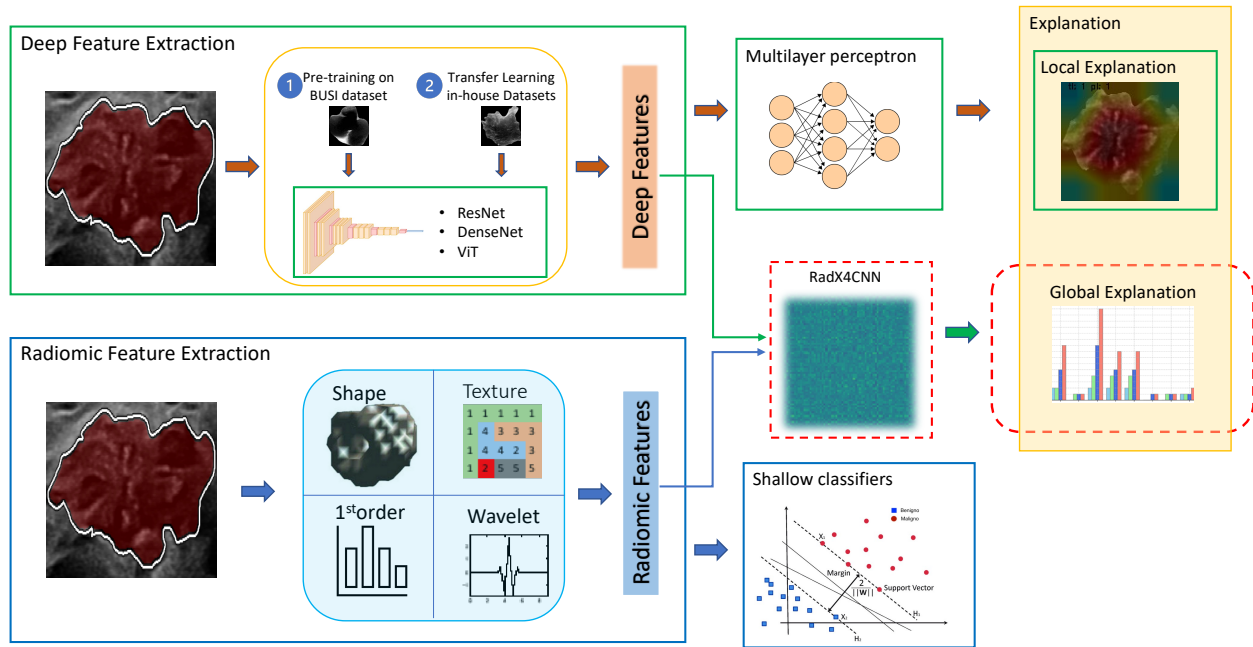


Figure 1: Overall workflow. Deep and Radiomic approaches were implemented for feature extraction and classification. Successively, radiomic and deep features were employed for Rad4XCNN implementation, providing a global explanation method.

[2016a]. GradCAM Selvaraju et al. [2017] has been introduced after CAM, to overcome the limitation of being able to visualize only the last layer and only particular CNN architectures. Despite many other methods being proposed later, GradCAM is still one of the most popular. Lately, *gradient-free* methods are also gaining wide popularity to overcome some limitations for computing gradients in very-deep architectures, and overcome the problem of anomalous behavior in incorrect prediction scenarios Muhammad and Yeasin [2020].

Saliency maps are mainly used to provide local explanations and it is not clear how these tools can be used for global explanation. Furthermore, it is important to emphasize that criticisms have been raised about their use Prinzi et al. [2023a]. According to Oh et al. [2020], Signoroni et al. [2021], for instance, poorly localized and spatially blurred vision was discovered in certain instances. Furthermore, it has been demonstrated that various methods for computing saliency maps can yield contradictory outcomes Prinzi et al. [2024a], Zhang et al. [2022].

2.3 Explainability in Radiomics

Radiomics is gaining prominence for extracting features from radiological images. It operates on the premise that some pixel-wise patterns are hidden from the human eye Gillies et al. [2016]. In contrast to deep features, radiomic features quantify certain properties like texture/pattern and statistical measurement by applying mathematical formulas to the images. For this reason, radiomic features are also called *hand-crafted*, counterposed to the *learned* extracted by neural networks. Radiomic flow has several advantages over deep extraction. Radiomic feature extraction does not require a large amount of data, as is the case with deep feature extraction Wei [2021]. Moreover, shallow learning algorithms prove to be well-suited for classifying radiomic data, widely recognized as more appropriate for training with small datasets. The primary benefit of radiomic features is their inherent interpretability, as their meanings are well understood Militello et al. [2023], Prinzi et al. [2024b]. Using shallow learning algorithms alongside these inherently interpretable features allows for both local and global explanations of the predictive models.

2.4 Our Rationale

Despite in some applications the use of transparent models can be sufficient Rudin [2019], the design of a transparent model can introduce a level of complexity Chen et al. [2022]: deep features tend to be more informative than interpretable radiomic features. In addition, the use of transparent algorithms (such as linear models) may fail when the relationships between the data are complex and nonlinear. As a consequence, the use of transparent-by-design models can lead to

poor performance. For this reason, the eternal conflict between the explainability and accuracy trade-off comes into play.

The literature indicates the need for new methods for CNN explanation that deviate from those based on visualization maps Papanastasiou et al. [2023]. Some attempts have been made by Paul et al. [2019], Wang et al. [2019], Chen et al. [2016] although there is no explicit reference to XAI. Paul et al. [2019] evaluated how radiomic model performance varies by replacing a correlated deep feature in the radiomic signature. However, regarding the performed interpretable feature extraction, the Image Biomarkers Standardization Initiative (IBSI) guidelines Zwanenburg et al. [2020] had not yet been proposed at that time. As a consequence, assessing the reproducibility of the study and the resulting impact of the study can be challenging. In addition, the authors do not use state-of-the-art deep extraction architectures such as ResNet, DenseNet, and ViT, whose depth is quite different from the VGG employed. Furthermore, they agree with an important limitation regarding the fact that a single slice was used to extract deep features in a volumetric image, whereas semantic information was generated from multiple slices. Above all, in contrast to our idea, they modify the input signature by replacing semantic features with deep ones, introducing a kind of constraint for model training. Wang et al. [2019] attempts to exploit the radiologist’s knowledge to qualitatively and visually correlate CNN-based feature maps with semantic features related to the investigated domain. However, these radiological features are operator-dependent, as is their correlation with the feature maps. As a result, their proof-of-concept is not generalizable to any context or domain. A similar idea was proposed in Chen et al. [2016], to reduce the gap between deep features and various clinical semantic features. The model aims to yield semantic rating scores to support a deeper analysis for either clinical diagnosis or educational purposes. More recently, Liu et al. [2023] tried to train deep models to grade informative semantic features related to the analyzed task rather than directly predicting the disease malignancy. Both papers lack formalism regarding the terminology related to explainable AI (*i.e.*, the characteristics of the method in terms of global-local explanation, applicability, class dependencies, etc.) In general, in the attempt to make the predictive process transparent, the cited articles, employ semantic features subject to inter-operator variability or modify the training process, which could harm the established predictive performance of deep models.

In this paper, we present Rad4XCNN, a method that integrates deep features’ predictive strengths with the interpretability of radiomic features. The method does not introduce any constraints in the training that can inhibit its accuracy. Considering the development of new explanation methods not solely based on visualization maps as a major challenge Papanastasiou et al. [2023], Rad4XCNN offers an innovative approach to explain deep architectures and provides a global explanation of deep networks, an aspect often overlooked in current research.

3 Materials and Methods

Figure 1 shows the flow diagram of the proposed method. For the deep workflow ResNet50, DenseNet121, and ViT-B32 were pre-trained on the BUSI dataset. Then transfer learning was implemented using the two in-house datasets. The extracted deep features were employed both for classification (via multilayer perceptron) and for explanation (local explanation via visualization maps). For the radiomic workflow, radiomic features were extracted, preprocessed, and used to train shallow classifiers. Radiomic and deep features were used as input for Rad4XCNN providing a global explanation.

3.1 Datasets Description

Breast Ultrasound Images Dataset (BUSI) - The BUSI Al-Dhabyani et al. [2020] comprises 780 ultrasound images obtained from 600 patients aged 25-75 years in 2018, alongside corresponding masks in PNG format. The images, containing the Focal Breast Lesions (FBLs) and measuring 500×500 pixels, are categorized into three classes: benign, malignant, and normal. Among these, 438 images present benign lesions, 211 are malignant, and 133 are classified as normal. Normal samples were not used in the study. The dataset exhibits class imbalance, with 67.49% (438 images) benign and 32.51% (211 images) malignant samples.

Table 1 provides the details concerning the number of images available of the BUSI dataset before and after the data augmentation, which was performed to increase the training set of the minority class: only the malignant class was augmented. Moreover, the table reports the dataset subdivision for training, validation, and test phases. After the initial 80:20 ratio between ‘Training/Validation’ and ‘Test’, the ‘Training/Validation’ set was again divided by applying an 80:20 ratio to obtain the ‘Training’ and ‘Validation’ sets.

Palermo and Cefalù Datasets - Two *in-house* datasets were collected on two centers, referred to as *Palermo* and *Cefalù* datasets. Considering the Palermo site, 237 breast cancer patients were enrolled in 2021 at Policlinico Universitario “P. Giaccone”. This dataset was employed for model tuning and internal test. Instead, considering the Cefalù site, 115 breast cancer patients were enrolled in 2022 at Fondazione Istituto “G. Giglio” Breast Unit. This dataset

Table 1: Details concerning the number of images available of the BUSI dataset before and after the data augmentation, which was performed to increase the training set of the minority class. Moreover, the table reports the dataset subdivision for training, validation, and test phases. (*) indicates the number of images obtained after data augmentation.

Lesion Class	Training/Validation (80%)			Test (20%)
	Training (80%)		Validation (20%)	
	before data augmentation	after data augmentation		
Benign	280	280	70	88
Malignant	135	270 (*)	34	42
Total	415	550	104	130

Table 2: Description of the in-house collected dataset, coming from Palermo and Cefalù hospitals.

Characteristic	Palermo Dataset	Cefalù Dataset
image size	845 × 600	845 × 600
focal breast lesions	237	115
benign lesion	132	70
malignant lesion	105	45
size range [mm]	4-90	3-50
mean size [mm]	15.12 ± 9.44	14.64 ± 8.61
age range [years]	17-88	23-89
mean age [years]	53.15 ± 15.00	51.61 ± 14.56

was used only for model external validation. Table 2 provides a detailed explanation of the in-house datasets. FBL images of both datasets were acquired through the B-mode ultrasound modality. Two expert breast radiologists (one from each institution with over 30 years of expertise in breast imaging) used two identical ultrasound RS85 (Samsung Medison, Co. Ltd.) devices, each with a 3–12 MHz linear transducer. Acquired FBLs were labeled using the ultrasound BI-RADS criteria Sickles and D’Orsi [2014], and successively the images were segmented. The adopted inclusion criteria for our breast ultrasound in-house datasets are discussed here Bartolotta et al. [2021]. Patients had not received any intervention or surgery on lesions before the ultrasound examination. Lack of biopsy or irregular follow-up were the exclusion criteria Bartolotta et al. [2024]. Table 3 shows the split of the proprietary datasets used for training and testing. A cross-validation was implemented using the training set.

3.2 Deep Architecture Training

This section includes a description of the workflow used to train deep architectures. In particular, preprocessing strategies, data preparation for training and test, and the implemented architectures are discussed. In addition, state-of-the-art methods for deep features explanation were exposed as well as our novel Rad4XCNN method. The diagram reported in Figure 2 depicts the details about the training, the testing, and the external validation related to deep workflow.

Table 3: Details on proprietary datasets: splits employed for model training and test.

Lesion Class	Palermo Dataset			Cefalù Dataset
	Total	Training	Test	Test
Benign	132	106	26	70
Malignant	105	84	21	45
Total	237	190	47	115

Image preprocessing - Tumor patches were extracted from the whole image using the available masks. All patches were resized to size 128×128 , specifically: *i*) images with a size larger than 128×128 were subsampled, and *ii*) zero-padding was applied to images with a smaller size. Images were normalized before model training.

Training and test protocol - Using an 80:20 ratio, the BUSI dataset was split into training and test sets. With the same ratio, the training set was divided once more into training and validation sets. Whereas having unbalanced datasets can lead to models affected by bias Hasib et al. [2020], the training set was balanced by considering random flip, rotation, contrast enhancement, translation, and zoom. The purpose of the BUSI dataset, in light of the recent criticism Pawłowska et al. [2023], was to produce an optimized pre-trained model solely. Regarding the Palermo dataset, 20% was used as an independent test set, while the remaining 80% was used to implement a 5-fold cross-validation (CV). The Cefalù dataset was used only for external validation. The best model in terms of accuracy within the CV procedure was selected for the Palermo internal test and the Cefalù external validation.

Saliency Maps Computation - Saliency maps highlight regions of an input image that most contribute to the prediction. Considering a classification task with c classes and a convolutional neural network with A^k feature map activations, Grad-CAM Selvaraju et al. [2017] is formalized as:

$$L_{Grad-CAM}^c = ReLU\left(\sum_k \alpha_k^c A_l^k\right) \quad (1)$$

where:

$$\alpha_k^c = \frac{1}{z} \sum_i \sum_j \frac{\partial y^c}{\partial A_{ij}^k} \quad (2)$$

Here $\frac{1}{z} \sum_i \sum_j$ represents the global average pooling operator over the width and height dimensions (indexed by i and j respectively) and $\frac{\partial y^c}{\partial A_{ij}^k}$ gradients via backpropagation. The weights α_k^c reflect a partial linearization and quantify feature map k importance for a given target class c . Grad-CAM's dependence on class c makes it a class discriminative method. Although Grad-CAM appears as one of the most widely used approaches, has two main limitations related to the gradient computation: *i*) saturation: The zero-gradient area of the ReLU function or the saturation problem for the Sigmoid function may cause the gradient to vanish; and *ii*) false confidence: when compared to a zero baseline, activation maps with larger weights exhibit smaller contributions to the network's output Wang et al. [2020]. Furthermore, backpropagating any quantity has extra computing overhead and relies on the assumption that classifiers generated accurate prediction; in the event that an incorrect decision is made, all of the aforementioned techniques will result in inaccurate or distorted representations Muhammad and Yeasin [2020].

Score-CAM introduced the Channel-wise Increase of Confidence (CIC), in contrast to Grad-CAM Selvaraju et al. [2017], which uses the gradient information coming into the last convolutional layer to reflect the relevance of each activation map Wang et al. [2020].

$$L_{Score-CAM}^c = ReLU\left(\sum_k \alpha_k^c A_l^k\right) \quad (3)$$

with:

$$\alpha_k^c = C(A_l^k) \quad (4)$$

where the CIC, used to gauge each activation map's significance, is shown by the symbol $C(\cdot)$.

EigenCAM is a gradient-free method and uses the principal components from the extracted feature maps Muhammad and Yeasin [2020]. For this reason, it can overcome the problem of distorted displays in case of incorrect predictions. Let $W_{L=k}$ represent the combined weight matrix of the first k layers of size (m, n) , and let I represent the input image of size $(i \times j)$, $I \in \mathbb{R}^{i \times j}$. The image I projected onto the last convolution layer $L = k$ is the class-activated output, and it is provided by $O_{L=k} = W_{L=k}^T I$. The principal components of $O_{L=k}$ can be computed by factorizing $O_{L=k}$ using singular value decomposition, which yields $O_{L=K} = U \Sigma V^T$. Σ is a diagonal matrix of size $M \times N$ with singular values along the diagonal, and V are the left singular vectors. U is an orthogonal matrix of size $M \times M$, and the left

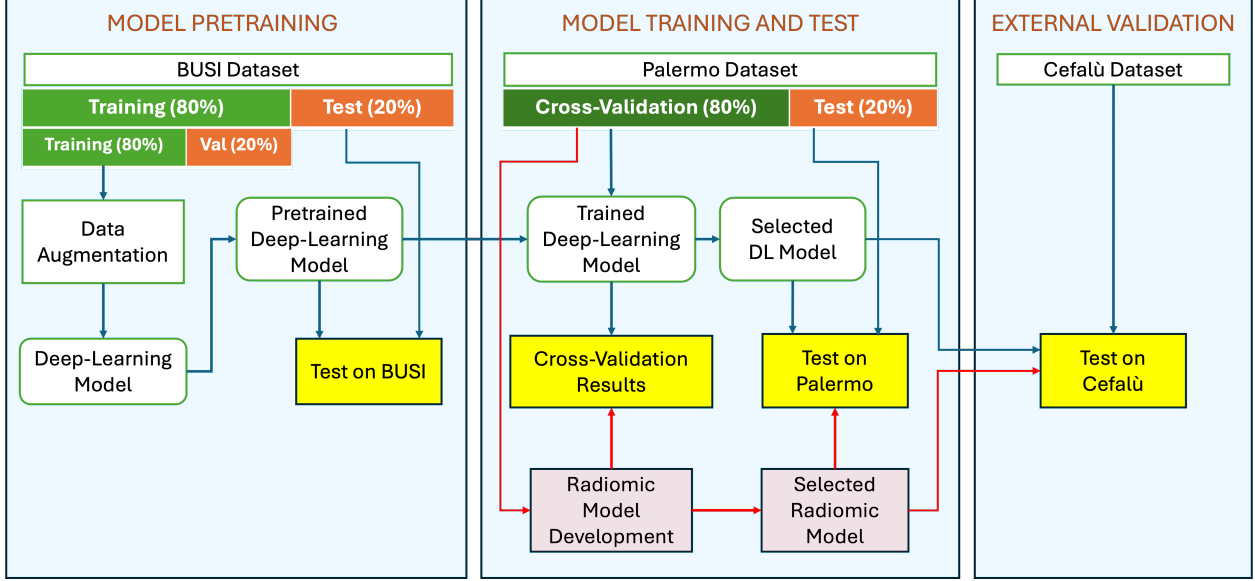


Figure 2: Diagram depicting the details about the training, the testing, and the external validation related to deep and radiomic workflow.

singular vectors are found in the column U . The projection of $O_{L=k}$ on the first eigenvector yields the class activation map:

$$L_{EigenCAM} = O_{L=k} V_1 \quad (5)$$

where the first eigenvector in the V matrix is V_1 . Eigen-CAM is class-independent, *e.g.* the result of saliency maps is not tied to any class.

The three methods (*e.g.* Grad-CAM, Score-CAM, and Eigen-CAM) were implemented to compare the different explanations provided and, thus, highlight existing gaps and the need for alternative explanation techniques.

3.3 Radiomic Models Training

Radiomic workflow includes ROI segmentation, feature extraction, feature preprocessing, selection, and model training. The diagram reported in Figure 2, already introduced in the previous section, depicts the details about the training, the testing, and the external validation related to radiomic workflow.

ROI Segmentation - Radiologists used S-DetectTM to perform ROI segmentation from each B-mode image of the breast lesion. Installed on the RS85 ultrasound machine, this software is licensed for clinical usage and is available for purchase.

Feature Extraction - PyRadiomics Van Griethuysen et al. [2017] is a toolkit that complies with the IBSI Zwanenburg et al. [2020], and was used to extract a total of 474 radiomic features. By standardizing the radiomic analysis procedure, IBSI increases workflow reproducibility. Extracted features belong to the following categories: shape 2D; first-order intensity histogram statistics; Gray Level Co-occurrence Matrix features (GLCM); Gray Level Run Length Matrix (GLRLM); Gray Level Size Zone Matrix (GLSZM); Gray Level Dependence Matrix (GLDM); Neighboring Gray Tone Difference Matrix (NGTDM). Features were extracted discretizing images to 255 gray levels. Furthermore, considering the high productivity of wavelet-derived radiomic features in comparison to the original ones Prinzi et al. [2023b], non-shape features were extracted also considering the Haar wavelet transform.

Features Preprocessing and Selection - Non-redundant and informative features were selected Militello et al. [2022], Papanikolaou et al. [2020] through: *i*) near-zero variance analysis to eliminate features with poor information content (variance cutoff $\sigma^2 = 0.005$); *ii*) correlation analysis to exclude strongly correlated features (the Spearman correlation with a 0.9 threshold value was evaluated). Eventually, the Sequential Feature Selector (SFS) algorithm was employed in

conjunction with the Random Forest (RF), XGBoost (XGB), and Support Vector Machine (SVM) classifiers. Accuracy was used as a metric to maximize.

Predictive Model Setup - This study employed three distinct shallow classifiers: RF, XGB, and SVM. These algorithms have proven suitable for tabular data in small dataset scenarios Prinzi et al. [2022]. RF and XGB were trained using 100 estimators. For XGB a learning rate of 0.3 and gain as the importance type were employed. SVM was trained using RBF kernel and features were standardized. A stratified 10-fold Cross-Validation approach that was repeated 20 times was taken into consideration. To perform the test phase, the model with the highest accuracy after 20 repetitions of a 10-fold cross-validation process was selected.

3.4 Deep Features Explanation by means of Radiomics

Rad4XCNN aims to explain the deep features extracted through the intrinsic meaning of radiomic features. Let $f_r = (r_1, r_2, \dots, r_a)$ denote the radiomic features, and $f_d = (d_1, d_2, \dots, d_b)$ denote the deep features, where a and b are the number of radiomic and deep features, respectively. The method assumes the use of a correlation index, and Spearman’s test was employed in this work. The Spearman correlation coefficient between f_r and f_d is given by:

$$\rho_{i,j} = \frac{\text{cov}(r_i, d_j)}{\sigma_r \sigma_d} \forall i \in [1, a], j \in [1, b], \text{ with } i, j \in \mathbb{N} \quad (6)$$

where: $\text{cov}(r_i, d_j)$ is the covariance between r_i and d_j , σ_r is the standard deviation of r_i , σ_d is the standard deviation of d_j .

To explain the meaning of f_d exploiting the correlation with the features f_r using a thresholds M , a threshold function $T(\rho, M)$ is defined such that:

$$T(\rho, M) = \begin{cases} 1 & \text{if } \rho \geq M \\ 0 & \text{otherwise} \end{cases} \quad (7)$$

where: ρ is the Spearman correlation coefficient between f_r and f_d , M is the threshold value. M represents a method hyperparameter to be determined according to the specific case study. By applying different threshold values, it is possible to determine which features in f_d are correlated with radiomic features f_r . It assumed that correlated radiomic and deep features describe the same phenomenon (*e.g.* features have a similar meaning) Paul et al. [2019], Wang et al. [2019]. Below are the main characteristics of the proposed method:

Global Explanation - Our method implements the notion of global explanation, diverging from approaches reliant on computing saliency maps, which constitute a form of local explanation. Global explanation is a key aspect of clinical model validation as it facilitates a comparative analysis of model findings against the existing clinical literature.

Model-agnostic - This method is agnostic, making it universally applicable across architectures and application contexts. It merely necessitates the extraction of feature vectors f_d and f_r , rendering it adaptable to any model and application without constraints. In agreement with the other saliency maps methods, Rad4XCNN need the vectorized version f_d of features maps A_{ij}^k , such as Grad-CAM, Score-CAM and $W_{L=k}$ Eigen-CAM.

Class-Independent - Rad4XCNN explains deep features without class specificity, such as Eigen-CAM. Conversely, it contrasts with Grad-CAM and Score-CAM, which are class-dependent considering the computation of α_k^c .

Ease of Implementation - It requires only the extraction of f_d , which is inherently part of any training process, along with the extraction of radiomic features f_r and the subsequent calculation of their correlation. The simplicity of implementation is the basis of several widely adopted and popular techniques Muhammad and Yeasin [2020], Zeiler and Fergus [2014].

4 Experimental Results

Deep models were trained using Adam optimizer and 8 as batch size. For ResNet50 and DenseNet121 10^{-4} was used as the learning rate, and 10^{-5} for ViT. A rate of 0.5 was used for dropout layers. The BUSI dataset was employed to obtain an initial pre-trained model, and 80% of the Palermo dataset was used for fine-tuning. Then, the remaining 20% of the Palermo dataset was used as an internal test, and the whole Cefalù dataset for external validation.

Table 4: Cross-validation performance comparison of VGG, ResNet, ViT, and the radiomic model on the Palermo training dataset.

Model	Acc	AUROC	Sens	Spec	PPV	NPV
ResNet50	93.62 ± 9.19	0.95 ± 0.09	91.20 ± 14.83	96.26 ± 4.6	95.23 ± 5.91	93.01 ± 12.00
DenseNet121	93.17 ± 13.66	0.94 ± 0.12	93.33 ± 13.33	93.00 ± 14.00	93.33 ± 13.33	93.00 ± 14.00
ViT-B32	93.65 ± 11.5	0.97 ± 0.6	92.16 ± 12.95	95.00 ± 10.00	94.74 ± 10.53	92.80 ± 12.42
Rad + XGB	61.49 ± 9.88	0.65 ± 0.10	53.63 ± 16.79	67.53 ± 14.13	56.63 ± 13.19	66.05 ± 9.59
Rad + RF	59.93 ± 9.19	0.60 ± 0.11	39.61 ± 14.31	75.35 ± 13.01	56.66 ± 17.76	62.10 ± 7.34
Rad + SVM	65.05 ± 8.31	0.62 ± 0.10	55.83 ± 15.05	72.09 ± 12.13	61.52 ± 10.06	68.70 ± 8.60

Table 5: Internal test and external validation performance using ResNet, DenseNet, ViT, and radiomic models on the Palermo and Cefalù test datasets.

Model	Palermo Hospital Dataset						Cefalù Hospital Dataset					
	Acc	AUROC	Sens	Spec	PPV	NPV	Acc	AUROC	Sens	Spec	PPV	NPV
ResNet50	72.22	0.733	66.67	76.19	66.67	76.19	73.04	0.757	77.78	70.00	62.5	83.05
DenseNet121	77.78	0.784	73.33	80.95	73.33	80.95	70.44	0.755	68.89	71.43	60.78	78.13
ViT-B32	83.33	0.848	93.33	76.19	73.68	94.12	62.61	0.742	77.78	52.86	51.47	78.72
Rad + XGB	47.22	0.43	46.15	47.82	33.33	47.22	61.11	00.60	60.86	61.35	62.89	60.86
Rad + RF	58.33	0.61	61.15	56.52	44.44	58.33	51.12	0.55	54.78	53.47	56.25	54.78
Rad + SVM	58.33	0.58	53.84	60.86	43.75	58.33	58.17	0.62	58.26	58.08	60.09	58.26

4.1 Deep and Radiomic Models Performance

Table 4 provides a comparison between radiomic and deep models considering the Palermo training dataset. ResNet50, DenseNet121, and ViT-B32, demonstrate remarkable performance compared to radiomic models. ResNet achieves an impressive accuracy of 93.62% ± 9.19 and AUROC of 0.95 ± 0.09, showcasing its robustness in classification tasks. Similarly, DenseNet and ViT exhibit high accuracies and AUROC scores, proving the dominance of deep learning-based approaches over radiomic models. In contrast, models incorporating radiomic features coupled with traditional machine learning algorithms such as XGB, RF, and SVM perform poorly compared to deep architectures.

Internal test and external validation performance are shown in Table 5, in which again the superiority of deep models over radiomic-based approaches is shown. In the Palermo dataset, ResNet achieves an accuracy of 72.22% and AUROC of 0.733, while DenseNet and ViT achieve even higher accuracies and AUROC scores. These results highlight the effectiveness of deep learning methodologies in extracting meaningful features from the datasets, leading to improved diagnostic performance. On the Cefalù dataset, a similar trend is observed, with deep models outperforming radiomic-based approaches. In particular, ResNet proved the best generalization capability on the external validation, showing an accuracy of 73.04% and a good balance between sensitivity and specificity. It is important to emphasize that although the performance of ResNet on the internal test is much lower than ViT, on the external validation ResNet maintains its performance, as opposed to ViT which achieves a heavy degradation. For this reason, we consider ResNet the best-trained model, and further considerations on explainability are provided for ResNet.

In contrast, models incorporating radiomic features combined with traditional machine learning algorithms consistently demonstrate inferior performance compared to deep learning models on both internal test and external validation datasets. These results underscore the limitations of radiomic-based approaches in capturing complex patterns and features present in medical images, particularly when compared to the feature extraction capabilities of deep learning architectures.

4.2 Traditional CNN Explainability

As the most accurate model in the external validation, ResNet was selected to analyze the traditional explainability methods based on saliency maps. By comparing the saliency maps obtained with GradCAM, EigenCAM, and ScoreCAM methods, it is possible to observe conflicting results among these interpretability techniques. Figure 3 shows some examples. Despite ResNet’s robust performance, the interpretations provided by these methods often diverged, presenting a challenge in understanding the model decision. This discrepancy raises questions about the reliability and consistency of these interpretability methods, urging a closer examination of their underlying mechanisms. Similar

inconsistencies are recently achieved in Cerekci et al. [2024], Zhang et al. [2022]. In particular, Rows 1-2 show two examples of correctly classified lesions, while Rows 3-4 show two examples of wrongly classified lesions. Some explanations predominantly focused on background regions, even when the model’s prediction was correct. Other concerns arise in the case of wrong prediction. Considering Grad-CAM, this effect is due to the dependence of the gradient calculation of $\frac{\partial y^c}{\partial A_{k_j}^c}$ (see Equation 2) that is a function of the prediction y^c , assumed correctly predicted the class c . For Score-CAM this problem is mitigated by CIC which weights the importance of each activation map. For Eigen-CAM decomposition does not depend on the predicted class and gradient computation. This phenomenon underlines the complexity of interpreting neural network decisions and highlights the need for newer interpretability techniques capable of overcoming these problems and providing clearer and more actionable insights.

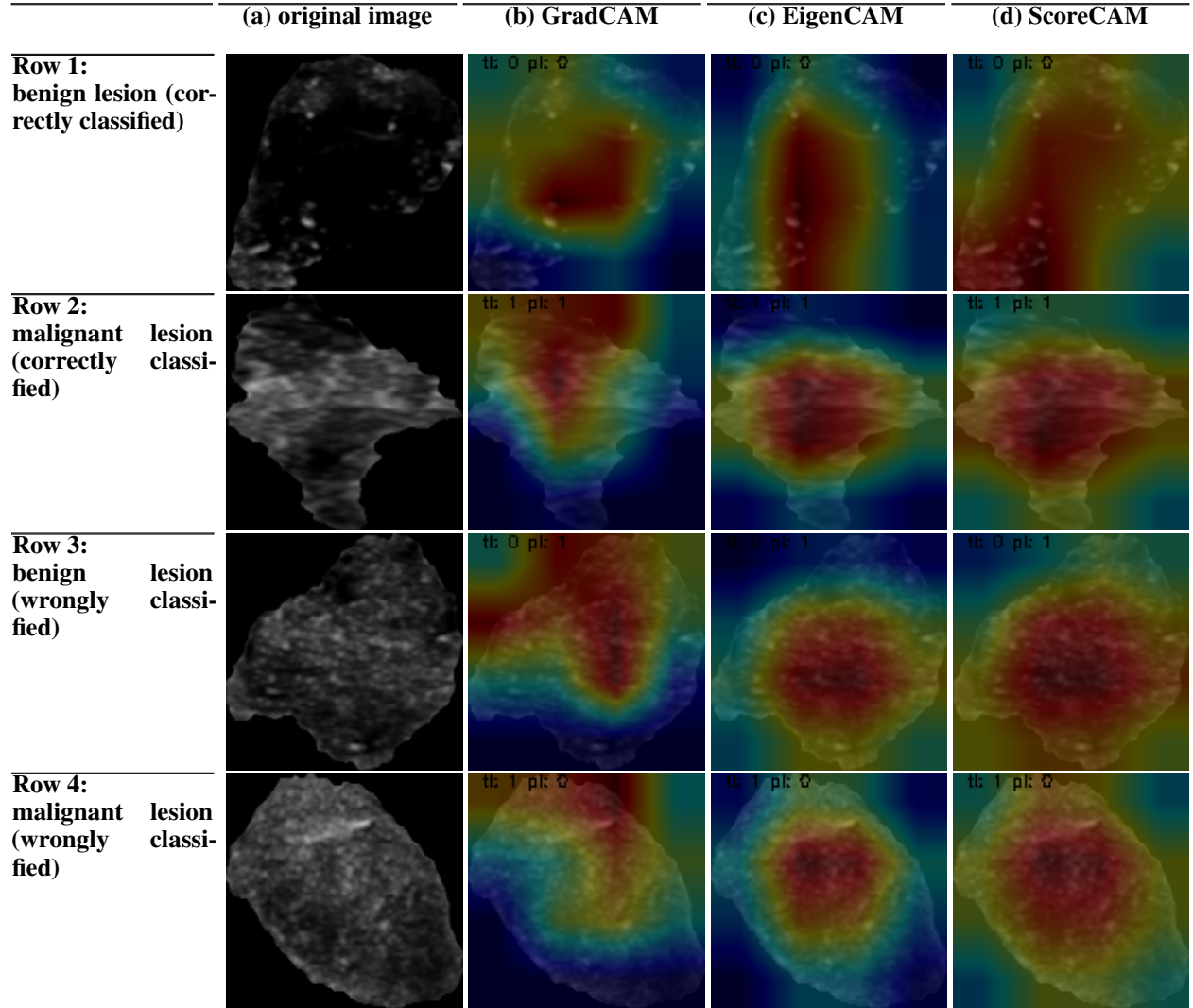


Figure 3: (a) original ultrasound image; (b) ultrasound image with overlapped the GradCAM saliency map; (c) ultrasound image with overlapped the EigenCAM saliency map; (d) ultrasound image with overlapped the ScoreCAM saliency map.

4.3 Explaining Deep Features by means of Radiomics in Ultrasound Breast Dataset

Figure 4 depicts the Rad4XCNN results, utilizing four distinct threshold values $\rho = [0.30, 0.35, 0.40, 0.45]$. The graph exclusively illustrates correlations with deep features derived from convolutional networks, as no correlations were identified with features extracted from VITs. Regarding the CNN-derived features (extracted from ResNet), our analysis reveals that *Energy*, and *TotalEnergy* emerge as the most prominently correlated features, with 15 correlations observed at a threshold of 0.3, 9 at 0.35, 4 at 0.4, and 2 at 0.45. Additionally, a high correlation (with $\rho = 0.45$) was established

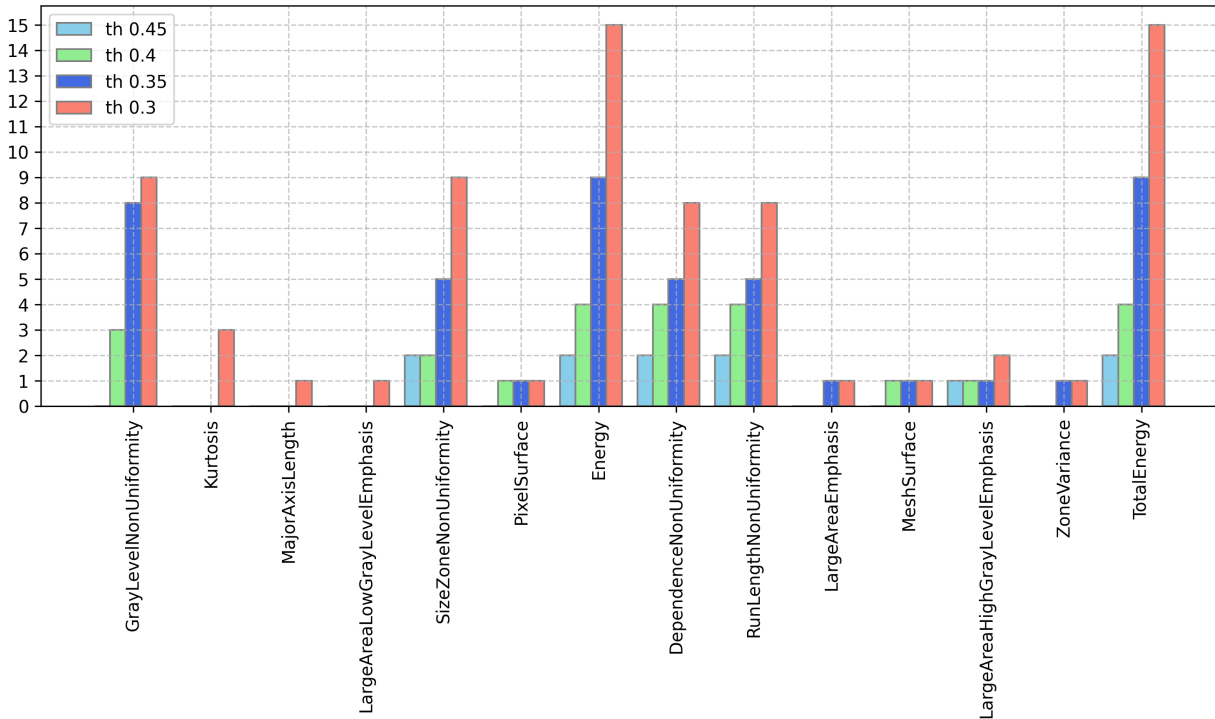


Figure 4: Global explanation of CNN-derived features obtained using Rad4XCNN. Each bar represents the number of CNN-derived features showing a correlation with radiomic features. The Y-axis reports the number of deep features correlated with the radiomic feature specified in the X-axis.

with *SizeZoneNonUniformity*, *DependenceNonUniformity*, and *RunLengthNonUniformity*. These 5 radiomic features (*i.e.* *Energy*, *TotalEnergy*, *SizeZoneNonUniformity*, *DependenceNonUniformity*, and *RunLengthNonUniformity*) collect all the correlations, both those with the original (unfiltered) version of the feature and those derived after filtering (considering the wavelets, with the 4 decompositions).

These correlations pave the way for pertinent clinical discussions, with implications already resonating within clinical practice. Further exploration of these clinical considerations is undertaken in Section 5.4.

5 Discussion

The concept of XAI is attracting much interest Holzinger et al. [2019], Stogiannos et al. [2023] and is playing a key role in the implementation and deployment of eXplainable Clinical Decision Support Systems (X-CDSSs). In this perspective, our work introduces several novelties. Rad4XCNN does not impose any methodological constraints that can harm the model performance to introduce explainability. In addition, it is agnostic, *e.g.* it is possible to apply it to any CNN-based architecture. Our findings allowed us *i)* to find a substantial difference between radiomic, CNN-derived, and ViT-derived features, in terms of accuracy and explainability; *ii)* to analyze some concerns related to the field of XAI, which our method attempts to mitigate; *iii)* to highlight important clinical aspects in the context of breast cancer that are consistent with the clinical literature.

5.1 Comparing ViT-derived, CNN-derived and Radiomic Features

Rad4XCNN enabled an analysis of the role of radiomic, CNN-derived, and ViT-derived features, in terms of accuracy, explainability, and intrinsic meaning of deep features.

In terms of performance - The ability of deep architectures to extract high and low-level features makes deep features much more informative than radiomic ones. As a consequence, many works have shown that approaches exploiting deep features achieve higher performance than radiomics Lisson et al. [2022], Sun et al. [2020], Truhn et al.

[2019], Wei [2021]. In our case, considering the evaluation on the external validation, CNN-derived features enabled higher accuracy compared with ViT-derived (5). Regardless of datasets, ResNet maintains high accuracy values.

In terms of explainability - Saliency maps generated through GradCAM, EigenCAM, and ScoreCAM can effectively emphasize meaningful areas for prediction. While they serve as valuable visual and qualitative aids for prediction analysis, two primary concerns are presented: *i*) each method yields distinct explanations, indicating a need for cautious interpretation; *ii*) these methods can lead to inter-operator variability evaluation, as individual physicians may interpret the explanations differently; *iii*) these explanations are inherently local, posing challenges to extract global insights. In contrast, radiomic features offer clearer and more comparable explanations. Since it is possible to associate each radiomic feature with meaning/behavior related to its analytical definition, they enable the comparison of features identified in other studies with those observed in clinical practice.

Comparing CNN-derived and ViT-derived features - As highlighted in Section 4.3, a notable alignment was observed between CNN-derived and radiomic features, whereas none was found with those extracted from ViT. This outcome aligns intuitively with an examination of the internal structures of the two architectures. CNN-based approaches typically rely on hierarchical feature extraction through a series of convolutional and pooling layers, capturing local patterns and spatial dependencies within the image. In contrast, ViT architectures adopt a self-attention mechanism, enabling them to capture global context by considering relationships between all image patches simultaneously. This leads CNNs to excel at capturing fine-grained details and local structures while ViTs in modeling long-range dependencies and contextual understanding. The authors explicitly admit that some intrinsic biases present in convolutional neural networks—such as translation equivariance and locality—are absent from transformers Dosovitskiy et al. [2020]. This similarity between radiomic features and CNN-derived features arises from their shared principle of extracting local characteristics. Convolutional filters in CNNs capture local information through the Receptive Field kernels and a hierarchical structure of layers. Likewise, radiomic features are predominantly derived from matrices that analyze the relationships among gray levels of adjacent pixels. This common approach aligns CNN-derived features closely with radiomic features, setting them apart from ViT-derived features. For these reasons, we consider Rad4XCNN as a global explanation method to explain CNN-derived features.

5.2 Explainability Properties of Rad4XCNN

Rad4XCNN offers a distinct perspective by explaining deep features through associations with the intrinsic interpretable radiomic features. This approach enables a richer clinically relevant understanding that surpasses the limitations of activation map-based methods. The advantages of Rad4XCNN can be summarized as follows:

- **provides global explanations:** it enables global insights, facilitating the extraction of clinically meaningful patterns across the entire dataset. This global perspective is valuable for clinical applications, where understanding overarching trends is as critical as individual predictions;
- **uses intelligible features:** the interpretable nature of radiomic features allows radiologists to correlate them with established clinical and radiological knowledge. While activation maps highlight regions of interest and enable only a qualitative analysis, radiomic features offer quantitative insights, helping bridge model predictions with well-known clinical evidence;
- **maintains model accuracy without training constraints:** approaches try to overcome the explainability-accuracy trade-off (e.g., Self-Explaining Neural Networks) often encounter a trade-off between robustness and accuracy due to imposed architectural constraints Alvarez Melis and Jaakkola [2018]. In fact, a change in test accuracy was shown as robustness regularization increases Elbaghdadi et al. [2020]. As a result, these model categories increase robustness and explainability at the cost of accuracy. Other methods require a specific structure for their use. For example, traditional activation-based techniques such as CAM Zhou et al. [2016b], necessitate specific architectural configurations, like a Global Average Pooling layer before dense layers, limiting architecture flexibility. In contrast, Rad4XCNN allows the optimization of any CNN model using a standard training process. Then, in a *post-hoc* manner, the correlation between deep and radiomic features is computed, thus preserving model performance and flexibility across tasks. For this reason, Rad4XCNN *i*) achieves transparency without compromising predictive accuracy, *ii*) mitigates some concerns related to the explainability-accuracy trade-off, and *iii*) overcomes the accuracy-explainability trade-off dilemma.

5.3 Mitigating XAI Concerns Through Rad4XCNN

Explainable AI is a challenging branch that certainly provides substantial advantages over traditional AI-based approaches for X-CDSS development and implementation. However, although there has been a tendency to integrate

global and local model explanations into the conventional development pipeline, XAI has also raised some criticisms. In fact, it seems that in some circumstances, an explanation may have also negative effects: *i*) if the model displays less information, then excluding an explanation, users are not confused about the model (lower cognitive overload); *ii*) often, intrinsic explainability is weak, and users should be trained to understand the explanations; *iii*) it appears that end-users are more interested to understand '*what the system does*' rather than '*how the system works*' Bell et al. [2022]. However, some of the mentioned issues can be mitigated considering Rad4XCNN and are discussed below.

An Explanation Makes the Model Reliable? In our research, the significant inconsistencies in methods relying on saliency maps were confirmed, a finding corroborated by numerous other studies Cerekci et al. [2024], Prinzi et al. [2024a], Zhang et al. [2022]. Consequently, even though these methods can identify where a model focuses for prediction, their reliability remains doubtful Cerekci et al. [2024], Oh et al. [2020], Prinzi et al. [2023a, 2024a], Signoroni et al. [2021], Zhang et al. [2022]. As a result, it is impossible to state with certainty the reliability of the trained model and to extract certain clinical insights. Furthermore, the need to propose new methods beyond the visualization map-based methods was highlighted. Papanastasiou et al. [2023].

In light of this, we conducted a qualitative comparison of Rad4XCNN with three widely used saliency map generation methods, to prove Rad4XCNN reliability (see Figure 3). The exploited techniques in the comparison are among the most representative and widespread in the literature for explaining deep architecture predictions: GradCAM, is representative of a gradient-based method, while ScoreCAM and EigenCAM avoid gradient computation to overcome some GradCAM shortcomings. In this perspective, our results highlight the unreliability of the saliency map methods and comply with previous papers Zhang et al. [2022], Prinzi et al. [2024a]. In particular, regarding Figure 3 we can highlight two main concerns:

- *discrepancy*: the three methods return different explanations. In particular, for the image in Row 1, all the explanations differ. For the other images (Rows 2, 3, and 4), GradCAM explanation is deeply different from ScoreCAM and EigenCAM. This can negatively affect physician interpretation;
- *unreliability*: although the first two images (Rows 1 and 2) show correct predictions, explanations seem unreliable. In fact, saliency maps highlight the background as the most important part.

Rad4XCNN allows medical professionals to analyze whether radiomic features, whose significance is well defined, are aligned with the clinical literature. In addition, it is possible to extract new clinical findings, such as those discussed in Section 5.4. This aspect overcomes the human tendency towards a positive interpretation of results by choosing the solution they want to be the correct one Bornstein [2016], providing an objective explanation.

Accuracy and Explainability trade-off Dilemma - Achieving the trade-off between explainability and accuracy is still an open dilemma Bell et al. [2022]. Although this trade-off has been widely discussed, there are some experiments where it is highlighted that in the clinical context, a patient would prefer an accurate model rather than an explainable one van der Veer et al. [2021b]. This would suggest that one should never sacrifice accuracy for the sake of explainability. Considering the absence of a definitive solution to this question, Rad4XCNN refrains from imposing constraints on model training. Instead, it provides an approach where radiomic features, although less predictive than deep ones, are exclusively utilized for explanatory purposes. It remains a task of the deep model to perform prediction accurately.

Explaining apparently incomprehensible patterns - The abstraction mechanism within convolutional networks implies that the extracted features have a significantly higher level of abstraction than radiomic features. In this perspective, XAI methodologies must recognize that, although it is possible to explain model decisions, understanding the relationships identified by deep architectures may be inherently incomprehensible. However, Rad4XCNN elucidates that a correlation exists between CNN-derived and radiomic features, demonstrating a convergence between physician insights and AI-based interpretations, as highlighted in the following section.

5.4 Radiomics-based explanation and its clinical validation

The radiomic features, found to be correlated with the CNN-derived features (Figure 4), have already been used in literature breast cancer studies, both diagnostic and prognostic. It is worth noting that if a study identifies a specific feature as important, it allows for direct comparisons to analyze if the same feature holds significance in other studies. This is not feasible with only qualitative saliency maps. Radiomic features, representing and quantifying the manifestation of the underlying tumor phenotype, can be considered biomarkers to be integrated into clinical practice. As a result, they offer a quantitative basis for influencing clinical decision-making. For example, in the study by Cui et al. [2023] on the link between ultrasound radiomic features and biological functions in the prediction of HER2 status in breast cancer, Size Zone Non-Uniformity (SZNU) feature was associated with 1,871 genes in 75

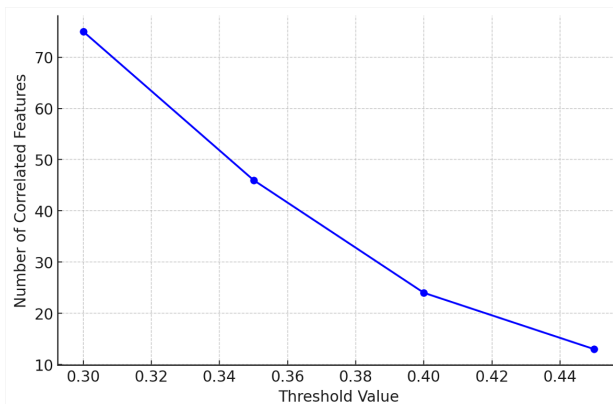


Figure 5: Correlation trend between radiomic and deep features.

perturbations and with carbon metabolism in cancer regarding biological functions; another radiomic feature analyzed in the same study Cui et al. [2023] was Run Length Non-Uniformity (RLNU), associated with the cell cycle and intercellular communication. In the study by Youk *et al.* on the analysis of the ultrasound radiomic features in benign and malignant breast masses Youk et al. [2020], 22 grayscale radiomic features were selected, some of which are also used in our study, such as Kurtosis, Energy, Run Length non-uniformity. The *energy*-derived features such as *Energy* and *Total Energy* are closely related to the intensity of gray levels. These features were found crucial in several studies related to breast cancer, such as the proposed one, and in DCE-MRI, in which a strong correlation is present with the temporal evolution of the contrast agent Prinzi et al. [2024c]. These radiomic features describe the change in gray intensity after administration of contrast medium, which is more rapid in malignant lesions, so these latter shows a more rapid increase in energy, *viceversa* for benign lesions. In breast ultrasound evaluation, excluding completely anechoic lesions, gray levels related to the echogenicity of a focal lesion may vary, but most malignant lesions are hypoechoic Rahbar et al. [1999]. Although the correlation between gray level intensity and the malignant lesion is different in DCE-MRI than in ultrasonographic features, even in ultrasonographic radiomic analysis, we can assert that both Energy and Total Energy emerge as characterizing features in ultrasonography, thereby laying a solid foundation for subsequent clinical investigations. The significance of signal intensity in ultrasound has been demonstrated in various anatomical districts Papini et al. [2002], Tessler et al. [2017], indicating its potential importance for breast imaging as well. Another example is the correlation between lesion heterogeneity, habitats' presence, and malignancy Marusyk and Polyak [2010], Diaz-Cano [2012]. The entropy is a quantity that measures the degree of disorder in a system. Among radiomic features, *entropy* is directly proportional to the heterogeneity of the lesion 'system' (*e.g.* due to prominent vascularization and presence of different types of cells) and thus its malignancy.

As a consequence, Rad4XCNN, by establishing a link between deep features and related radiomic features that can be interpreted from a radiological point of view, can reduce the gap between black-box models and the explainability properties required by radiologists. Our results confirm an interesting overlap between the radiomics features and radiologist insights. This enables deep features to be considered clinical biomarkers such as radiomic features, with the advantage of obtaining more performing models. The missing link in this chain - the correlation between deep features and radiomics - is provided by Rad4XCNN. To provide more detail on this last aspect, Figure 5 depicts the correlation trend.

5.5 Clinical Implications of Rad4XCNN Use

Rad4XCNN contributes to improving current clinical practices in the radiologic domain. In particular, three main aspects were addressed:

- **model clinical validation through quantitative radiomic features:** Rad4XCNN stands out for its focus on clinical validation, using quantitative radiomic variables that provide an objective and measurable view of image global characteristics, allowing for more accurate and reproducible radiologist-based assessment. This aspect is essential for model reliability;
- **reduction of inter-operator variability in interpreting model findings:** Rad4XCNN improves model explanation, overcoming the qualitative interpretation of saliency maps, which may be subject to inter-operator variability. As a result, Rad4XCNN enhances clinicians' trust and facilitates the adoption of predictive models into everyday workflows;

- **integration of intelligible features within the clinical practice:** The integration of radiomic features into the interpretation of medical images provides an added layer of confidence in results validation. Radiologists can now combine traditional image analysis with the richness of radiomic features. This fusion enhances clinical decision-making and enhances the traditional reporting process with new possible features to use as biomarkers.

5.6 Rad4XCNN Limitations

From a methodological perspective, Rad4XCNN application requires ROIs segmentation for radiomic feature extraction. In contrast, deep learning models typically automatically learn the most important features (the ROI is not needed). In particular, for Rad4XCNN, it is crucial to have pre-defined segmentation of ROIs to ensure that radiomic features are extracted solely from pathological areas, avoiding irrelevant information from surrounding healthy tissue. However, although segmentation is a resource-intensive process, several tools are available nowadays for accurate and rapid segmentation. From a clinical perspective, it is essential for radiologists to understand the meaning of each radiomic feature to derive clinical insights accurately. While the number of extracted features is often substantial, radiomic features have become increasingly standardized and are now being widely incorporated into clinical literature. Furthermore, feature extraction software is typically accompanied by detailed documentation, making it easier for non-experts to comprehend and utilize these features effectively.

6 Conclusion

In this study, we have presented Rad4XCNN, a novel approach for the development of eXplainable Clinical Decision Support Systems, bridging the gap between accuracy and explainability without imposing methodological constraints on model performance. Through a comprehensive analysis comparing radiomic, Convolutional Neural Network (CNN)-derived, and Vision Transformer (ViT)-derived features in the context of breast cancer diagnosis, we have shed light on several critical aspects of XAI and its application in clinical decision-making.

Our findings highlight significant differences between radiomic, CNN-derived, and ViT-derived features in terms of accuracy and explainability. While deep architectures, particularly CNNs, demonstrate superior performance in terms of accuracy, radiomic features offer clearer and more comparable explanations due to their well-defined significance. Rad4XCNN revealed a notable alignment between CNN-derived and radiomic features, indicating shared principles of extracting local characteristics. Moreover, we addressed concerns surrounding XAI through Rad4XCNN, offering insights into its reliability, the accuracy-explainability trade-off dilemma, and the complexity of deep model explanations. By identifying radiomic features that exhibit a high correlation with CNN-derived features we were able to draw some important clinical conclusions. The correlation between these features and those observed in previous studies on breast cancer diagnosis underscores the clinical relevance and potential utility of our findings.

A promising future research direction would be exploring how this approach could be extended to explain features derived from ViTs, given the different feature extraction processes compared to CNNs. Additionally, incorporating structured semantic information, such as BI-RADS attributes (*e.g.*, density, margin shape, microcalcifications, etc.), could further enrich model interpretability. These attributes could serve dual purposes: *i*) improving classification accuracy and *ii*) enabling the association of global intelligible features with extracted deep features. This exploration could open up new pathways for aligning deep learning features with clinically recognized descriptors, facilitating more meaningful insights in medical image analysis.

Summarizing, the use of Radiomics in CNN explanation represents a promising advancement in the development of XCDSSs. It provides a new perspective on XAI methods that deviate from the methods based on visualization maps. In addition, it provides a form of global explanation, an aspect often overlooked in current research on explainable methods in medical imaging.

Ethics Statement

The study was approved by the Ethical Committee of the Policlinico University Hospital ‘P. Giaccone’ of Palermo (minute N. 02/2019 of 18/02/2019). Informed consent was waived because of the retrospective nature of the study and the analysis. The data of the patients involved were processed according to the institutional privacy regulations of the Policlinico University Hospital ‘P. Giaccone’ of Palermo. The privacy rights of the human subjects involved in the study are respected because anonymized clinical and imaging data were used.

CRedit authorship contribution statement

Francesco Prinzi: conceptualization, methodology, software, formal analysis, writing original draft, visualization; **Carmelo Militello**: conceptualization, methodology, formal analysis, writing original draft, visualization; **Calogero Zarcaro**: validation, investigation, data curation; **Tommaso Vincenzo Bartolotta**: validation, investigation, data curation, supervision; **Salvatore Gaglio**: validation, investigation, writing - review and editing, supervision; **Salvatore Vitabile**: validation, investigation, resources, writing - review and editing, supervision, project administration, funding acquisition.

Funding

This research was *i*) funded by the Italian Complementary National Plan PNC-I.1 "Research initiatives for innovative technologies and pathways in the health and welfare sector" D.D. 931 of 06/06/2022, "DARE - DigitAI lifelong pRevEntion" initiative, code PNC0000002, CUP: B53C22006460001; and *ii*) funded by the European Union – Next Generation EU - Progetti di Ricerca di Rilevante Interesse Nazionale (PRIN) 2022, Prot. 2022ENK9LS. Project: "EXEGETE: Explainable Generative Deep Learning Methods for Medical Image and Signal Processing", CUP: B53D23013040006.

Acknowledgments

The authors would like to thank Dr. Alice Latino for their substantial contribution to some experiments.

References

- Shinjini Kundu. Ai in medicine must be explainable. *Nature medicine*, 27(8):1328–1328, 2021. doi:10.1038/s41591-021-01461-z.
- Alejandro Barredo Arrieta, Natalia Díaz-Rodríguez, Javier Del Ser, Adrien Bennetot, Siham Tabik, Alberto Barbado, Salvador García, Sergio Gil-López, Daniel Molina, Richard Benjamins, et al. Explainable artificial intelligence (xai): Concepts, taxonomies, opportunities and challenges toward responsible ai. *Information fusion*, 58:82–115, 2020. doi:10.1016/j.inffus.2019.12.012.
- Andrew Smith. Using artificial intelligence and algorithms. *Federal Trade Commission*, 2020.
- Riccardo Guidotti, Anna Monreale, Salvatore Ruggieri, Franco Turini, Fosca Giannotti, and Dino Pedreschi. A survey of methods for explaining black box models. *ACM computing surveys (CSUR)*, 51(5):1–42, 2018. doi:10.1145/3236009.
- European Community. Artificial Intelligence Act. <https://artificialintelligenceact.eu/the-act/>, 2024. Accessed: 2024-12-10.
- Cecilia Panigutti, Ronan Hamon, Isabelle Hupont, David Fernandez Llorca, Delia Fano Yela, Henrik Junklewitz, Salvatore Scalzo, Gabriele Mazzini, Ignacio Sanchez, Josep Soler Garrido, et al. The role of explainable ai in the context of the ai act. In *Proceedings of the 2023 ACM conference on fairness, accountability, and transparency*, pages 1139–1150, 2023. doi:10.1145/3593013.3594069.
- Julia Amann, Alessandro Blasimme, Effy Vayena, Dietmar Frey, Vince I Madai, and Precise4Q Consortium. Explainability for artificial intelligence in healthcare: a multidisciplinary perspective. *BMC medical informatics and decision making*, 20:1–9, 2020. doi:10.1186/s12911-020-01332-6.
- Carlo Combi, Beatrice Amico, Riccardo Bellazzi, Andreas Holzinger, Jason H Moore, Marinka Zitnik, and John H Holmes. A manifesto on explainability for artificial intelligence in medicine. *Artificial Intelligence in Medicine*, 133:102423, 2022. doi:10.1016/j.artmed.2022.102423.
- Andreas Holzinger. Interactive machine learning for health informatics: when do we need the human-in-the-loop? *Brain Informatics*, 3(2):119–131, 2016. doi:10.1007/s40708-016-0042-6.
- Andreas Holzinger, Georg Langs, Helmut Denk, Kurt Zatloukal, and Heimo Müller. Causability and explainability of artificial intelligence in medicine. *Wiley Interdisciplinary Reviews: Data Mining and Knowledge Discovery*, 9(4):e1312, 2019. doi:10.1002/widm.1312.
- Aaron M Bornstein. Is artificial intelligence permanently inscrutable. *Nautilus*, 40, 2016.
- Marzyeh Ghassemi, Luke Oakden-Rayner, and Andrew L Beam. The false hope of current approaches to explainable artificial intelligence in health care. *The Lancet Digital Health*, 3(11):e745–e750, 2021. doi:10.1016/S2589-7500(21)00208-9.

- Liam G McCoy, Connor TA Brenna, Stacy S Chen, Karina Vold, and Sunit Das. Believing in black boxes: machine learning for healthcare does not need explainability to be evidence-based. *Journal of clinical epidemiology*, 142: 252–257, 2022. doi:10.1016/j.jclinepi.2021.11.001.
- Alex John London. Artificial intelligence and black-box medical decisions: accuracy versus explainability. *Hastings Center Report*, 49(1):15–21, 2019. doi:10.1002/hast.973.
- Mlađan Jovanović and Mia Schmitz. Explainability as a user requirement for artificial intelligence systems. *Computer*, 55(2):90–94, 2022. doi:10.1109/MC.2021.3127753.
- Esma Aktufan Cerekci, Deniz Alis, Nurper Denizoglu, Ozden Camurdan, Mustafa Ege Seker, Caner Ozer, Muhammed Yusuf Hansu, Toygar Tanyel, Ilkay Oksuz, and Ercan Karaarslan. Quantitative evaluation of saliency-based explainable artificial intelligence (xai) methods in deep learning-based mammogram analysis. *European Journal of Radiology*, page 111356, 2024. doi:10.1016/j.ejrad.2024.111356.
- Francesco Prinzi, Marco Insalaco, Alessia Orlando, Salvatore Gaglio, and Salvatore Vitabile. A yolo-based model for breast cancer detection in mammograms. *Cognitive Computation*, 16(1):107–120, 2024a. doi:10.1007/s12559-023-10189-6.
- Jiajin Zhang, Hanqing Chao, Giridhar Dasegowda, Ge Wang, Mannudeep K Kalra, and Pingkun Yan. Overlooked trustworthiness of saliency maps. In *International Conference on Medical Image Computing and Computer-Assisted Intervention*, pages 451–461. Springer, 2022. doi:10.1007/978-3-031-16437-8_43.
- Francesco Prinzi, Carmelo Militello, Nicola Scichilone, Salvatore Gaglio, and Salvatore Vitabile. Explainable machine-learning models for COVID-19 prognosis prediction using clinical, laboratory and radiomic features. *IEEE Access*, 11:121492–121510, 2023a. doi:10.1109/ACCESS.2023.3327808.
- Robert J Gillies, Paul E Kinahan, and Hedvig Hricak. Radiomics: images are more than pictures, they are data. *Radiology*, 278(2):563–577, 2016. doi:10.1148/radiol.2015151169.
- Philippe Lambin, Ralph TH Leijenaar, Timo M Deist, Jurgen Peerlings, Evelyn EC De Jong, Janita Van Timmeren, Sebastian Sanduleanu, Ruben THM Larue, Aniek JG Even, Arthur Jochems, et al. Radiomics: the bridge between medical imaging and personalized medicine. *Nature reviews Clinical oncology*, 14(12):749–762, 2017. doi:10.1038/nrclinonc.2017.141.
- Francesco Prinzi, Alessia Orlando, Salvatore Gaglio, and Salvatore Vitabile. Interpretable radiomic signature for breast microcalcification detection and classification. *Journal of Imaging Informatics in Medicine*, 2024b. doi:10.1007/s10278-024-01012-1.
- Francesco Prinzi, Alessia Orlando, Salvatore Gaglio, and Salvatore Vitabile. Breast cancer classification through multivariate radiomic time series analysis in dce-mri sequences. *Expert Systems with Applications*, 249:123557, 2024c. doi:10.1016/j.eswa.2024.123557.
- Chansik An, Yae Won Park, Sung Soo Ahn, Kyunghwa Han, Hwiyoung Kim, and Seung-Koo Lee. Radiomics machine learning study with a small sample size: Single random training-test set split may lead to unreliable results. *PLoS One*, 16(8):e0256152, 2021. doi:10.1371/journal.pone.0256152.
- Alberto Traverso, Leonard Wee, Andre Dekker, and Robert Gillies. Repeatability and reproducibility of radiomic features: a systematic review. *International Journal of Radiation Oncology* Biology* Physics*, 102(4):1143–1158, 2018. doi:10.1016/j.ijrobp.2018.05.053.
- Catharina Silvia Lisson, Christoph Gerhard Lisson, Marc Fabian Mezger, Daniel Wolf, Stefan Andreas Schmidt, Wolfgang M Thaiss, Eugen Tausch, Ambros J Beer, Stephan Stilgenbauer, Meinrad Beer, et al. Deep neural networks and machine learning radiomics modelling for prediction of relapse in mantle cell lymphoma. *Cancers*, 14(8):2008, 2022. doi:10.3390/cancers14082008.
- Qiuchang Sun, Xiaona Lin, Yuanshen Zhao, Ling Li, Kai Yan, Dong Liang, Desheng Sun, and Zhi-Cheng Li. Deep learning vs. radiomics for predicting axillary lymph node metastasis of breast cancer using ultrasound images: don't forget the peritumoral region. *Frontiers in oncology*, 10:53, 2020. doi:10.3389/fonc.2020.00053.
- Daniel Truhn, Simone Schrading, Christoph Haarbuerger, Hannah Schneider, Dorit Merhof, and Christiane Kuhl. Radiomic versus convolutional neural networks analysis for classification of contrast-enhancing lesions at multiparametric breast mri. *Radiology*, 290(2):290–297, 2019. doi:10.1148/radiol.2018181352.
- Peng Wei. Radiomics, deep learning and early diagnosis in oncology. *Emerging topics in life sciences*, 5(6):829–835, 2021. doi:10.1042/ETLS20210218.
- Giulia Varriano, Pasquale Guerriero, Antonella Santone, Francesco Mercaldo, and Luca Brunese. Explainability of radiomics through formal methods. *Computer Methods and Programs in Biomedicine*, 220:106824, 2022. doi:10.1016/j.cmpb.2022.106824.

- Leonardo Rundo and Carmelo Militello. Image biomarkers and explainable ai: handcrafted features versus deep learned features. *European Radiology Experimental*, 8:130, 2024. doi:10.1186/s41747-024-00529-y.
- Sabine N van der Veer, Lisa Riste, Sudeh Cheraghi-Sohi, Denham L Phipps, Mary P Tully, Kyle Bozentko, Sarah Atwood, Alex Hubbard, Carl Wiper, Malcolm Oswald, et al. Trading off accuracy and explainability in ai decision-making: findings from 2 citizens' juries. *Journal of the American Medical Informatics Association*, 28(10):2128–2138, 2021a. doi:10.1093/jamia/ocab127.
- Md Atiqur Rahman, Mustavi Ibne Masum, Khan Md Hasib, MF Mridha, Sultan Alfarhood, Mejdil Safran, and Dunren Che. Gliomacnn: An effective lightweight cnn model in assessment of classifying brain tumor from magnetic resonance images using explainable ai. *CMES-Computer Modeling in Engineering & Sciences*, 140(3), 2024. doi:10.32604/cmcs.2024.050760.
- David Alvarez Melis and Tommi Jaakkola. Towards robust interpretability with self-explaining neural networks. *Advances in neural information processing systems*, 31, 2018.
- Omar Elbaghdadi, Aman Hussain, Christoph Hoenes, and Ivan Bardarov. Self explaining neural networks: A review with extensions. *Fairness, Accountability, Confidentiality and Transparency in AI*, 2020.
- Giorgos Papanastasiou, Nikolaos Dikaios, Jiahao Huang, Chengjia Wang, and Guang Yang. Is attention all you need in medical image analysis? a review. *IEEE Journal of Biomedical and Health Informatics*, 2023. doi:10.1109/JBHI.2023.3348436.
- Luca Longo, Mario Brcic, Federico Cabitza, Jaesik Choi, Roberto Confalonieri, Javier Del Ser, Riccardo Guidotti, Yoichi Hayashi, Francisco Herrera, Andreas Holzinger, et al. Explainable artificial intelligence (xai) 2.0: A manifesto of open challenges and interdisciplinary research directions. *Information Fusion*, page 102301, 2024. doi:10.1016/j.inffus.2024.102301.
- Bart M de Vries, Gerben JC Zwezerijnen, George L Burchell, Floris HP van Velden, Catharina Willemien Menke-van der Houven van Oordt, and Ronald Boellaard. Explainable artificial intelligence (xai) in radiology and nuclear medicine: a literature review. *Frontiers in medicine*, 10:1180773, 2023. doi:10.3389/fmed.2023.1180773.
- Laurent Itti, Christof Koch, and Ernst Niebur. A model of saliency-based visual attention for rapid scene analysis. *IEEE Transactions on Pattern Analysis and Machine Intelligence*, 20(11):1254–1259, 1998. doi:10.1109/34.730558.
- Michail Mamalakis, Heloise de Vareilles, Atheer AI-Manea, Samantha C Mitchell, Ingrid Arartz, Lynn Egeland Morch-Johnsen, Jane Garrison, Jon Simons, Pietro Lio, John Suckling, et al. A 3d explainability framework to uncover learning patterns and crucial sub-regions in variable sulci recognition. *arXiv preprint arXiv:2309.00903*, 2023. doi:10.48550/arXiv.2309.00903.
- Karen Simonyan, Andrea Vedaldi, and Andrew Zisserman. Deep inside convolutional networks: Visualising image classification models and saliency maps. *arXiv preprint arXiv:1312.6034*, 2013. doi:10.48550/arXiv.1312.6034.
- Mukund Sundararajan, Ankur Taly, and Qiqi Yan. Axiomatic attribution for deep networks. In *International conference on machine learning*, pages 3319–3328. PMLR, 2017.
- Matthew D Zeiler, Graham W Taylor, and Rob Fergus. Adaptive deconvolutional networks for mid and high level feature learning. In *2011 international conference on computer vision*, pages 2018–2025. IEEE, 2011. doi:10.1109/ICCV.2011.6126474.
- Matthew D Zeiler and Rob Fergus. Visualizing and understanding convolutional networks. In *Computer Vision—ECCV 2014: 13th European Conference, Zurich, Switzerland, September 6–12, 2014, Proceedings, Part I 13*, pages 818–833. Springer, 2014. doi:10.1007/978-3-319-10590-1_53.
- Jost Tobias Springenberg, Alexey Dosovitskiy, Thomas Brox, and Martin Riedmiller. Striving for simplicity: The all convolutional net. *arXiv preprint arXiv:1412.6806*, 2014. doi:10.48550/arXiv.1412.6806.
- Bolei Zhou, Aditya Khosla, Agata Lapedriza, Aude Oliva, and Antonio Torralba. Learning deep features for discriminative localization. In *Proceedings of the IEEE conference on computer vision and pattern recognition*, pages 2921–2929, 2016a.
- Ramprasaath R Selvaraju, Michael Cogswell, Abhishek Das, Ramakrishna Vedantam, Devi Parikh, and Dhruv Batra. Grad-cam: Visual explanations from deep networks via gradient-based localization. In *Proceedings of the IEEE international conference on computer vision*, pages 618–626, 2017.
- Mohammed Bany Muhammad and Mohammed Yeasin. Eigen-cam: Class activation map using principal components. In *2020 international joint conference on neural networks (IJCNN)*, pages 1–7. IEEE, 2020. doi:10.1109/IJCNN48605.2020.9206626.
- Yujin Oh, Sangjoon Park, and Jong Chul Ye. Deep learning covid-19 features on cxr using limited training data sets. *IEEE Transactions on Medical Imaging*, 39(8):2688–2700, 2020. doi:10.1109/TMI.2020.2993291.

- Alberto Signoroni, Mattia Savardi, Sergio Benini, Nicola Adami, Riccardo Leonardi, Paolo Gibellini, Filippo Vaccher, Marco Ravanelli, Andrea Borghesi, Roberto Maroldi, et al. Bs-net: Learning covid-19 pneumonia severity on a large chest x-ray dataset. *Medical Image Analysis*, 71:102046, 2021. doi:10.1016/j.media.2021.102046.
- Carmelo Militello, Francesco Prinzi, Giulia Sollami, Leonardo Rundo, Ludovico La Grutta, and Salvatore Vitabile. Ct radiomic features and clinical biomarkers for predicting coronary artery disease. *Cognitive Computation*, 15(1): 238–253, 2023. doi:10.1007/s12559-023-10118-7.
- Cynthia Rudin. Stop explaining black box machine learning models for high stakes decisions and use interpretable models instead. *Nature machine intelligence*, 1(5):206–215, 2019. doi:10.1038/s42256-019-0048-x.
- Haomin Chen, Catalina Gomez, Chien-Ming Huang, and Mathias Unberath. Explainable medical imaging ai needs human-centered design: guidelines and evidence from a systematic review. *npj Digital Medicine*, 5(1):156, 2022. doi:10.1038/s41746-022-00699-2.
- Rahul Paul, Matthew Schabath, Yoganand Balagurunathan, Ying Liu, Qian Li, Robert Gillies, Lawrence O Hall, and Dmitry B Goldgof. Explaining deep features using radiologist-defined semantic features and traditional quantitative features. *Tomography*, 5(1):192–200, 2019. doi:10.18383/j.tom.2018.00034.
- Clinton J Wang, Charlie A Hamm, Lynn J Savic, Marc Ferrante, Isabel Schobert, Todd Schlachter, MingDe Lin, Jeffrey C Weinreb, James S Duncan, Julius Chapiro, et al. Deep learning for liver tumor diagnosis part ii: convolutional neural network interpretation using radiologic imaging features. *European radiology*, 29:3348–3357, 2019. doi:10.1007/s00330-019-06214-8.
- Sihong Chen, Jing Qin, Xing Ji, Baiying Lei, Tianfu Wang, Dong Ni, and Jie-Zhi Cheng. Automatic scoring of multiple semantic attributes with multi-task feature leverage: a study on pulmonary nodules in ct images. *IEEE Transactions on Medical Imaging*, 36(3):802–814, 2016. doi:10.1109/TMI.2016.2629462.
- Alex Zwanenburg, Martin Vallières, Mahmoud A Abdallah, Hugo JWL Aerts, Vincent Andrearczyk, Aditya Apte, Saeed Ashrafinia, Spyridon Bakas, Roelof J Beukinga, Ronald Boellaard, et al. The image biomarker standardization initiative: standardized quantitative radiomics for high-throughput image-based phenotyping. *Radiology*, 295(2): 328–338, 2020. doi:10.1148/radiol.2020191145.
- Caixia Liu, Ruibin Zhao, and Mingyong Pang. Semantic characteristic grading of pulmonary nodules based on deep neural networks. *BMC Medical Imaging*, 23(1):156, 2023. doi:10.1186/s12880-023-01112-4.
- Walid Al-Dhabyani, Mohammed Gomaa, Hussien Khaled, and Aly Fahmy. Dataset of breast ultrasound images. *Data in Brief*, 28:104863, 2020. doi:10.1016/j.dib.2019.104863.
- Edward A Sickles and Carl J D’Orsi. How should screening breast US be audited? the BI-RADS perspective. *Radiology*, 272(2):316–320, 2014. doi:10.1148/radiol.14140634.
- Tommaso Vincenzo Bartolotta, Alessia Angela Maria Orlando, Maria Laura Di Vittorio, Francesco Amato, Mariangela Dimarco, Domenica Matranga, and Raffaele Ienzi. S-detect characterization of focal solid breast lesions: a prospective analysis of inter-reader agreement for us bi-rads descriptors. *Journal of ultrasound*, 24:143–150, 2021. doi:10.1007/s40477-020-00476-5.
- Tommaso Vincenzo Bartolotta, Carmelo Militello, Francesco Prinzi, Fabiola Ferraro, Leonardo Rundo, Calogero Zarcaro, Mariangela Dimarco, Alessia Angela Maria Orlando, Domenica Matranga, and Salvatore Vitabile. Artificial intelligence-based, semi-automated segmentation for the extraction of ultrasound-derived radiomics features in breast cancer: a prospective multicenter study. *La radiologia medica*, pages 1–12, 2024. doi:10.1007/s11547-024-01826-7.
- Khan Md Hasib, Md Sadiq Iqbal, Faisal Muhammad Shah, Jubayer Al Mahmud, Mahmudul Hasan Popel, Md Imran Hossain Showrov, Shakil Ahmed, and Obaidur Rahman. A survey of methods for managing the classification and solution of data imbalance problem. *arXiv preprint arXiv:2012.11870*, 2020. doi:10.48550/arXiv.2012.11870.
- Anna Pawłowska, Piotr Karwat, and Norbert Żolek. Letter to the editor. re: “[dataset of breast ultrasound images by w. al-dhabyani, m. gomaa, h. khaled & a. fahmy, data in brief, 2020, 28, 104863]”. *Data in Brief*, 48:109247, 2023. ISSN 2352-3409. doi:10.1016/j.dib.2023.109247.
- Haofan Wang, Zifan Wang, Mengnan Du, Fan Yang, Zijian Zhang, Sirui Ding, Piotr Mardziel, and Xia Hu. Score-cam: Score-weighted visual explanations for convolutional neural networks. In *Proceedings of the IEEE/CVF conference on computer vision and pattern recognition workshops*, pages 24–25, 2020.
- Joost JM Van Griethuysen, Andriy Fedorov, Chintan Parmar, Ahmed Hosny, Nicole Aucoin, Vivek Narayan, Regina GH Beets-Tan, Jean-Christophe Fillion-Robin, Steve Pieper, and Hugo JWL Aerts. Computational radiomics system to decode the radiographic phenotype. *Cancer research*, 77(21):e104–e107, 2017. doi:10.1158/0008-5472.CAN-17-0339.

- Francesco Prinzi, Carmelo Militello, Vincenzo Conti, and Salvatore Vitabile. Impact of wavelet kernels on predictive capability of radiomic features: A case study on COVID-19 chest X-ray images. *Journal of Imaging*, 9(2):32, 2023b. doi:10.3390/jimaging9020032.
- Carmelo Militello, Leonardo Rundo, Mariangela Dimarco, Alessia Orlando, Ildebrando D'Angelo, Vincenzo Conti, and Tommaso Vincenzo Bartolotta. Robustness analysis of DCE-MRI-derived radiomic features in breast masses: Assessing quantization levels and segmentation agreement. *Applied Sciences*, 12(11):5512, 2022. doi:10.3390/app12115512.
- Nikolaos Papanikolaou, Celso Matos, and Dow Mu Koh. How to develop a meaningful radiomic signature for clinical use in oncologic patients. *Cancer Imaging*, 20:1–10, 2020. doi:10.1186/s40644-020-00311-4.
- Francesco Prinzi, Alessia Orlando, Salvatore Gaglio, Massimo Midiri, and Salvatore Vitabile. ML-Based radiomics analysis for breast cancer classification in DCE-MRI. In Mufti Mahmud, Cosimo Ieracitano, M. Shamim Kaiser, Nadia Mammone, and Francesco Carlo Morabito, editors, *Applied Intelligence and Informatics*, pages 144–158. Springer Nature Switzerland, 2022. doi:10.1007/978-3-031-24801-6_11.
- N Stogiannos, H Bougias, E Georgiadou, S Leandrou, and P Papavasileiou. Analysis of radiomic features derived from post-contrast t1-weighted images and apparent diffusion coefficient (adc) maps for breast lesion evaluation: A retrospective study. *Radiography*, 29(2):355–361, 2023. doi:10.1016/j.radi.2023.01.019.
- Alexey Dosovitskiy, Lucas Beyer, Alexander Kolesnikov, Dirk Weissenborn, Xiaohua Zhai, Thomas Unterthiner, Mostafa Dehghani, Matthias Minderer, Georg Heigold, Sylvain Gelly, et al. An image is worth 16x16 words: Transformers for image recognition at scale. *arXiv preprint arXiv:2010.11929*, 2020. doi:10.48550/arXiv.2010.11929.
- Bolei Zhou, Aditya Khosla, Agata Lapedriza, Aude Oliva, and Antonio Torralba. Learning deep features for discriminative localization. In *Proceedings of the IEEE conference on computer vision and pattern recognition*, pages 2921–2929, 2016b.
- Andrew Bell, Ian Solano-Kamaiko, Oded Nov, and Julia Stoyanovich. It's just not that simple: an empirical study of the accuracy-explainability trade-off in machine learning for public policy. In *2022 ACM Conference on Fairness, Accountability, and Transparency*, pages 248–266, 2022. doi:10.1145/3531146.3533090.
- Sabine N van der Veer, Lisa Riste, Sudeh Cheraghi-Sohi, Denham L Phipps, Mary P Tully, Kyle Bozentko, Sarah Atwood, Alex Hubbard, Carl Wiper, Malcolm Oswald, et al. Trading off accuracy and explainability in ai decision-making: findings from 2 citizens' juries. *Journal of the American Medical Informatics Association*, 28(10):2128–2138, 2021b. doi:10.1093/jamia/ocab127.
- Hao Cui, Yue Sun, Dantong Zhao, Xudong Zhang, Hanqing Kong, Nana Hu, Panting Wang, Xiaoxuan Zuo, Wei Fan, Yuan Yao, et al. Radiogenomic analysis of prediction her2 status in breast cancer by linking ultrasound radiomic feature module with biological functions. *Journal of Translational Medicine*, 21(1):44, 2023. doi:10.1186/s12967-022-03840-7.
- Ji Hyun Youk, Jin Young Kwak, Eunjung Lee, Eun Ju Son, and Jeong-Ah Kim. Grayscale ultrasound radiomic features and shear-wave elastography radiomic features in benign and malignant breast masses. *Ultraschall in der Medizin-European Journal of Ultrasound*, 41(04):390–396, 2020. doi:10.1055/a-0917-6825.
- Guita Rahbar, Angela C Sie, Gail C Hansen, Jeffrey S Prince, Michelle L Melany, Handel E Reynolds, Valerie P Jackson, James W Sayre, and Lawrence W Bassett. Benign versus malignant solid breast masses: Us differentiation. *Radiology*, 213(3):889–894, 1999. doi:10.1148/radiology.213.3.r99dc20889.
- Enrico Papini, Rinaldo Guglielmi, Antonio Bianchini, Anna Crescenzi, Silvia Taccogna, Francesco Nardi, Claudio Panunzi, Roberta Rinaldi, Vincenzo Toscano, and Claudio M Pacella. Risk of malignancy in nonpalpable thyroid nodules: predictive value of ultrasound and color-doppler features. *The Journal of Clinical Endocrinology & Metabolism*, 87(5):1941–1946, 2002. doi:10.1210/jcem.87.5.8504.
- Franklin N Tessler, William D Middleton, Edward G Grant, Jenny K Hoang, Lincoln L Berland, Sharlene A Teefey, John J Cronan, Michael D Beland, Terry S Desser, Mary C Frates, et al. Acr thyroid imaging, reporting and data system (ti-rads): white paper of the acr ti-rads committee. *Journal of the American college of radiology*, 14(5):587–595, 2017. doi:10.1016/j.jacr.2017.01.046.
- Andriy Marusyk and Kornelia Polyak. Tumor heterogeneity: causes and consequences. *Biochimica et Biophysica Acta (BBA)-Reviews on Cancer*, 1805(1):105–117, 2010. doi:10.1016/j.bbcan.2009.11.002.
- Salvador J Diaz-Cano. Tumor heterogeneity: mechanisms and bases for a reliable application of molecular marker design. *International journal of molecular sciences*, 13(2):1951–2011, 2012. doi:10.3390/ijms13021951.